bioRxiv preprint doi: https://doi.org/10.1101/2020.05.28.122499; this version posted May 29, 2020. The copyright holder for this preprint (which was not certified by peer review) is the author/funder, who has granted bioRxiv a license to display the preprint in perpetuity. It is made available under aCC-BY-NC-ND 4.0 International license.

Title: Neurobiological underpinnings of rapid white matter plasticity during intensive reading instruction

Abbreviated title: Neurobiology of white matter plasticity

Authors: Elizabeth Huber[1], Aviv Mezer[2], Jason D. Yeatman[3,4]

[1]Institute for Learning and Brain Sciences and Department of Speech and Hearing Sciences, University of Washington, Seattle, WA, 98195

[2]Edmond & Lily Safra Center for Brain Sciences, The Hebrew University of Jerusalem, Jerusalem, Israel

[3]Graduate School of Education, Stanford University, Stanford, CA, 94305

[4]Division of Developmental-Behavioral Pediatrics, Stanford University School of Medicine, Stanford, CA, 95305.

Corresponding Author: Elizabeth Huber, ehuber@uw.edu

Conflict of Interest: The authors declare no financial or other conflict of interest.

Acknowledgements: This work was funded by NSF/BSF BCS #1551330/ #2015608, Eunice Kennedy Shriver National Institute of Child Health and Human Development Grant R01 HD09586101 and Jacobs Foundation Research Fellowship to JDY.

bioRxiv preprint doi: https://doi.org/10.1101/2020.05.28.122499; this version posted May 29, 2020. The copyright holder for this preprint (which was not certified by peer review) is the author/funder, who has granted bioRxiv a license to display the preprint in perpetuity. It is made available under aCC-BY-NC-ND 4.0 International license.

Abstract

Human white matter is remarkably plastic. Yet it is challenging to infer the biological underpinnings of this plasticity using non-invasive measurements like diffusion MRI. Here we capitalize on metrics derived from diffusion kurtosis imaging (DKI) to interpret previously reported changes in mean diffusivity throughout the white matter during an 8-week, intensive reading intervention. We then use an independent quantitative MRI measurement of R1 (1/T1 relaxation time) in the same white matter regions; since R1 closely tracks variation in myelin content, it provides complementary information about white matter microstructure. Behavioral measures, multi-shell diffusion MRI data, and quantitative T1 data were collected at regular intervals during the intervention in a group of 33 children with reading difficulties (7-12 years old), and over the same period in an age-matched non-intervention control group. Changes in DKI parameters modeled over the intervention were consistent with increased hindrance in the extra-axonal space, rather than a large-scale change in axon density and/or myelination. Supporting this interpretation, analysis of R1 values did not suggest a change in myelin, although R1 estimates were correlated with individual differences in reading skill. Together, these results suggest that large-scale changes in diffusivity observed over a short timescale during an intensive educational experience are most likely to reflect changes occurring in the extra-axonal space, in line with recent work highlighting the role of glial cells in experience-dependent plasticity and learning.

Keywords: Diffusion MRI; quantitative MRI; white matter modeling; plasticity; reading

bioRxiv preprint doi: https://doi.org/10.1101/2020.05.28.122499; this version posted May 29, 2020. The copyright holder for this preprint (which was not certified by peer review) is the author/funder, who has granted bioRxiv a license to display the preprint in perpetuity. It is made available under aCC-BY-NC-ND 4.0 International license.

Introduction

Experience can modify the microstructure of the white matter over remarkably short timescales (Taubert, Draganski et al. 2010, Blumenfeld-Katzir, Pasternak et al. 2011, Engvig, Fjell et al. 2012, Hofstetter, Tavor et al. 2013, Mamiya, Richards et al. 2016, Huber 2018). The majority of past work examining white matter plasticity in humans has relied on diffusion MRI (dMRI) and metrics derived from the diffusion tensor model (DTI; Basser et al., 1996; Beaulieu 2002), which are sensitive to myriad features of the white matter, including the number, size and branching of glial cells, the density and caliber of axons, the abundance of myelin, and the spatial arrangement of fibers within an imaging voxel (Basser and Pierpaoli 1996, Alexander, Lee et al. 2007, Walhovd, Johansen-Berg et al. 2014). The diffusion kurtosis model (DKI; Jensen et al., 2005) offers increased sensitivity to microstructural variation and, potentially, increased specificity, by modeling variation in the diffusion signal that is not considered by the tensor model (Cheung et al., 2009; Veraart et al., 2010; Steven et al., 2014), although DKI metrics (e.g., mean kurtosis, MK) are generally no more straightforward to interpret than those derived from DTI (e.g., mean diffusivity, MD). Thus, a challenge for diffusion MRI studies of white matter plasticity is to understand the neurobiological underpinnings of the observed changes in diffusion properties since a variety of distinct mechanisms could account for the data.

Over the last decade, a host of modeling approaches have been developed to exploit biologically informed priors in pursuit of a more accurate and interpretable parcellation of the diffusion signal (Jelescu and Budde 2017, Alexander, Dyrby et al. 2019). For example,

bioRxiv preprint doi: https://doi.org/10.1101/2020.05.28.122499; this version posted May 29, 2020. The copyright holder for this preprint (which was not certified by peer review) is the author/funder, who has granted bioRxiv a license to display the preprint in perpetuity. It is made available under aCC-BY-NC-ND 4.0 International license.

the recent white matter tract integrity (WMTI) model (Fieremans, Novikov et al. 2010, Fieremans, Jensen et al. 2011) builds on DKI by defining separable axonal and extra-axonal contributions to the diffusion signal, which are explicitly modeled to provide metrics such as axonal water fraction (AWF) and extra-axonal diffusivity. These parameters have previously been shown to be sensitive to individual differences in white matter as a function of age (Chang, Owen et al. 2015, Jelescu, Veraart et al. 2015, Genc, Malpas et al. 2017) and cognitive performance (Chung, Fieremans et al. 2018), as well as white matter pathology (Fieremans, Benitez et al. 2013, Benitez, Fieremans et al. 2014), including de-myelination (Falangola, Guilfoyle et al. 2014, Jelescu, Veraart et al. 2015, Guglielmetti, Veraart et al. 2016, Jelescu, Zurek et al. 2016, Kelm, West et al. 2016). With appropriate pre-processing, AWF and extra-axonal diffusivity are highly reliable, even given the constraints associated with data collection in young children (Huber 2018).

Microstructural modeling of the diffusion signal thus holds promise for illuminating the biological underpinnings of white matter development, pathology, and plasticity. However, even the most sophisticated models incorporate simplifying assumptions about the underlying tissue, and many require that the user to set constraints, such as the absolute or relative expected diffusivity of individual tissue compartments (Jelescu, Veraart et al. 2015). Although it is often possible to make principled choices, in some cases, the most appropriate set of model assumptions is still up for debate: For example, while the WMTI model has previously been validated under the assumption that extra-axonal diffusivity is greater than intra-axonal diffusivity (Guglielmetti, Veraart et al. 2016, Jelescu, Zurek et al. 2016), recent work suggests that the opposite assumption may be more appropriate (intra-

bioRxiv preprint doi: https://doi.org/10.1101/2020.05.28.122499; this version posted May 29, 2020. The copyright holder for this preprint (which was not certified by peer review) is the author/funder, who has granted bioRxiv a license to display the preprint in perpetuity. It is made available under aCC-BY-NC-ND 4.0 International license.

92 axonal greater than extra-axonal diffusivity: (Jespersen, Olesen et al. 2018, Kunz, da Silva
93 et al. 2018). Thus, even state-of-the-art modeling techniques may be open to multiple
94 interpretations and, while model parameters can be used to inform new linking hypotheses,
95 it is not possible to directly link changes in any one parameter to a specific change in tissue
96 biology.
97
98 Multi-modal studies that combine microstructural modeling with complementary
99 measurements, such as quantitative T1 mapping, can provide critical insight beyond what
100 can be gleaned from diffusion alone (Cercignani and Bouyagoub 2018, Filo, Shtangel et
101 al. 2019, Takemura, Ogawa et al. 2019, Travis, Castro et al. 2019). For example, in a large
102 cross-sectional study, complementary DTI and quantitative T1 relaxation measurements
103 showed distinct trajectories over the lifespan (Yeatman et al., 2014). Quantitative T1
104 measurements capture the interaction between tissue density and the chemical composition
105 of that tissue (Mezer, Yeatman et al. 2013, Stuber, Morawski et al. 2014, Filo, Shtangel et
106 al. 2019), such that T1 values are more attenuated in highly myelination regions, while
107 diffusion measurements are influenced by any cell membrane capable of hindering the
108 diffusion process(Le Bihan 1995). Thus, the authors reasoned that the discrepancy between
109 measures could reflect changes in various non-neuronal cell types (microglia,
110 oligodendrocyte precursor cells (OPC), and/or astrocytes). Such changes are presumed to
111 occur alongside changes in myelination, but with distinct dynamics over the lifespan.
112
113 Experience-dependent plasticity in the white matter likely depends on processes no less
114 complex than those unfolding over maturation and aging. Learning related changes in white

bioRxiv preprint doi: https://doi.org/10.1101/2020.05.28.122499; this version posted May 29, 2020. The copyright holder for this preprint (which was not certified by peer review) is the author/funder, who has granted bioRxiv a license to display the preprint in perpetuity. It is made available under aCC-BY-NC-ND 4.0 International license.

matter diffusivity could theoretically reflect a number of distinct biological phenomena, such as activity-dependent changes in myelination or glial cell proliferation (Blumenfeld-Katzir, Pasternak et al. 2011, Lerch, Yiu et al. 2011, Sagi, Tavor et al. 2012, Sampaio-Baptista, Khrapitchev et al. 2013, Gibson, Purger et al. 2014). In animal models, short-term learning has been associated both with remodeling of myelin and proliferation of glial cells in the gray and white matter (Blumenfeld-Katzir, Pasternak et al. 2011, Lerch, Yiu et al. 2011, Sagi, Tavor et al. 2012, Sampaio-Baptista, Khrapitchev et al. 2013). In the white matter, the size of non-axonal effects can even exceed subsequent changes in myelination (Gibson, Purger et al. 2014), which has been interpreted as reflecting an initial over-production of glial cells associated with the early stages of the learning process. Although non-invasive MRI measurements cannot directly specify the exact cellular changes that are occurring, they can be used to reason about the underlying biology of plasticity measured in the human brain, and they provide a vital link between the literature on human learning and invasive studies examining plasticity in other species.

We previously reported that 8 weeks of intensive reading instruction prompts widespread changes in white matter diffusion properties, which track the learning process (Huber 2018). Given that these effects occurred rapidly, and were distributed throughout the white matter, we speculated that the changes in diffusivity might reflect an initial stage of the learning process (e.g., large-scale glial cell proliferation), rather than changes to signal conduction properties of functionally relevant axons via changes in myelination or axon caliber. Here, we first confirmed that the previously reported finding of spatially distributed intervention-driven changes in diffusivity holds in a larger sample of subjects (n=33). We

bioRxiv preprint doi: https://doi.org/10.1101/2020.05.28.122499; this version posted May 29, 2020. The copyright holder for this preprint (which was not certified by peer review) is the author/funder, who has granted bioRxiv a license to display the preprint in perpetuity. It is made available under aCC-BY-NC-ND 4.0 International license.

then fit the WMTI model to these data to test for intervention-driven changes in the estimated axonal water fraction (AWF). Although we observed changes in diffusivity within the extra-axonal space, we failed to detect changes in AWF. We next explored how changing certain model assumptions affects the pattern of results in these data. Finally, we used an independent quantitative MRI measurement of R1 (1/T1 relaxation time) to examine the same white matter regions. Although R1 estimates were correlated with individual differences in reading skill, analysis of R1 values did not suggest a change in myelin content over the 8-week intervention period. Together, these results highlight the value of multi-modal MRI data for constraining inferences about underlying white matter biology, while pointing to the potential importance of non-neuronal cell types during the early stages of learning.

Materials and Methods

Participants

A total of 149 behavioral and MRI sessions were conducted with a group of 33 children ranging in age from 7 to 12 years, who participated in an intensive summer reading intervention program. Of these subjects, 24 were included in a previous manuscript (Huber 2018). Members of the intervention group were recruited based on parent report of reading difficulties and/or a clinical diagnosis of dyslexia. Multi-shell diffusion MRI and behavioral data were collected before the intervention (baseline), after 3.62 (+/- 0.16) weeks of intervention, after 6.71 (+/- 0.16) weeks of intervention, and at the end of the 8-

bioRxiv preprint doi: https://doi.org/10.1101/2020.05.28.122499; this version posted May 29, 2020. The copyright holder for this preprint (which was not certified by peer review) is the author/funder, who has granted bioRxiv a license to display the preprint in perpetuity. It is made available under aCC-BY-NC-ND 4.0 International license.

week intervention period. An additional 78 behavioral and MRI sessions were conducted with 29 participants, who were matched for age but not reading level. These subjects were recruited as a control group to assess the stability of our measurements over the repeated sessions. Control subjects participated in the same experimental sessions but did not receive the reading intervention. Some families of control group subjects were reluctant to commit to all four sessions, given that their children were not receiving an educational intervention. These families were given an opportunity to participate in 2 sessions. The interval for the two sessions was chosen in order to have balanced numbers of measurements at equivalent time points to the intervention group. In the intervention group, 5 subjects were unable to complete either the third of the fourth imaging session, and therefore participated in 3 sessions, total. The distribution of testing sessions for the intervention and control groups is summarized in **Table 1**.

	Baseline (0 days)	11-38	33-77	49-100
Intervention	33	33 (mean 25.36, std 6.70)	31 (mean 47.00, std 6.23)	30 (mean 72.70, std 10.91)
Control	29	20 (mean 22.25, std 6.51)	16 (mean 44.38, std 10.01)	12 (mean 58.33, std 5.31)

Table 1. Testing schedule for intervention and control groups. Experimental sessions were evenly spaced for each subject, with a baseline prior to the start of intervention, a second session within 11-38 days since the start of intervention (column 2), a third session within 33-77 days (column 3), and a fourth session within 49-100 days (column 4). Each cell gives the number of subjects sampled at each time bin. In the intervention group, some data sets are missing due to scheduling or data quality issues, while in the intervention group some subjects elected to complete only 2 sessions (see Methods for details). The mean number of days and standard deviation for each time bin are given in parenthesis.

bioRxiv preprint doi: https://doi.org/10.1101/2020.05.28.122499; this version posted May 29, 2020. The copyright holder for this preprint (which was not certified by peer review) is the author/funder, who has granted bioRxiv a license to display the preprint in perpetuity. It is made available under aCC-BY-NC-ND 4.0 International license.

All participants were native English speakers with normal or corrected-to-normal vision and no history of neurological damage or psychiatric disorder. Subjects were screened using a mock scanner to assess comfort and ability to hold still during the MRI sessions. We obtained written consent from parents, and verbal assent from all child participants. All procedures, including recruitment, consent, and testing, followed the guidelines of the University of Washington Human Subjects Division and were reviewed and approved by the UW Institutional Review Board. Subject demographics are given in **Table 2**.

	WJ-BRS	TOWRE	WJ-RF	WJ-CALC	WJ-MFF	Age (months)
Intervention	80.30/14.27	72.42/13.33	72.42/18.51	85.68/13.48	83.10/16.11	112.58/ 20.58
Control	96.55/19.59	86.74/22.31	91.74/22.33	97.45/13.72	92.67/18.00	117.03/ 14.38

Table 2. Demographic data for the intervention and non-intervention control groups. Each cell contains the group mean and standard deviation for a given item. Subject groups were matched in age but not reading skill. The first three columns give mean and standard deviation (mean / standard deviation) within each group for three standard reading measures: The Basic Reading Skill composite from the Woodcock Johnson Tests of Achievement (WJ-BRS), the Test of Word Reading Efficiency index (TOWRE), and The Reading Fluency subtest of the Woodcock Johnson Tests of Achievement (WJ-RF). Columns 4-5 give standard scores for the Woodcock Johnson Tests of Achievement Calculation (WJ-CALC) and Math Facts Fluency (WJ-MFF), which measure efficiency and accuracy of math related skills.

Reading intervention

bioRxiv preprint doi: https://doi.org/10.1101/2020.05.28.122499; this version posted May 29, 2020. The copyright holder for this preprint (which was not certified by peer review) is the author/funder, who has granted bioRxiv a license to display the preprint in perpetuity. It is made available under aCC-BY-NC-ND 4.0 International license.

Intervention subjects were enrolled in 8 weeks of the Seeing Stars: Symbol Imagery for Fluency, Orthography, Sight Words, and Spelling (Bell 2007) program at three different Lindamood-Bell Learning Centers in the Seattle area. The intervention program consists of directed, one-on-one training in phonological and orthographic processing skills, lasting four hours each day, five days a week. The curriculum uses an incremental approach, building from letters and syllables to words and connected texts, emphasizing phonological decoding skills as a foundation for spelling and comprehension. A hallmark of this intervention program is the intensity of the training protocol (4 hours a day, 5 days a week) and the personalized approach that comes with one-on-one instruction.

To test for longitudinal change in reading and non-reading (Calculation and Math Facts Fluency subtests of the Woodcock Johnson Tests of Achievement) measures, we fit a linear mixed effects model with a fixed effect of intervention time, in days (for control subjects, this corresponds to days since the baseline session), and a random effect of subject. The intervention group showed significant gains for all reading measures ($p < 0.05$ for WJ-BRS; $p < 0.0001$ for TOWRE and WJ-RF). We found no significant growth in the non-reading measures over the same time period. In a subset of reading-matched controls, who theoretically have as much room to improve on the reading measures as the intervention subjects (i.e., they are not approaching ceiling on the tests), we found no significant growth in any reading measure. Within this group, the math fluency (WJ-MFF) did improve with repeated testing ($p < 0.001$), presumably due to practice on the timed-test. Within the full control sample (including typical and highly skilled readers), performance on timed tests

bioRxiv preprint doi: https://doi.org/10.1101/2020.05.28.122499; this version posted May 29, 2020. The copyright holder for this preprint (which was not certified by peer review) is the author/funder, who has granted bioRxiv a license to display the preprint in perpetuity. It is made available under aCC-BY-NC-ND 4.0 International license.

(TOWRE, WJ-RF, and WJ-MFF) improved with repeated testing ($p < 0.01$), although reading accuracy (WJ-BRS) and calculation (WJ-CALC) showed no significant change.

Magnetic resonance imaging (MRI) acquisition protocol

All imaging data were acquired using a 3T Phillips Achieva scanner (Philips, Eindhoven, Netherlands) at the University of Washington Diagnostic Imaging Sciences Center (DISC) using a 32-channel head coil. An inflatable cap minimized head motion, and participants were continuously monitored through a closed-circuit camera system.

Diffusion-weighted magnetic resonance imaging (dMRI) data were acquired at 2.0mm^3 spatial resolution with full brain coverage. Each session consisted of 3 DWI scans, one with 32 non-collinear directions (b-value=800 s/mm^2), and a second with 64 non-collinear directions (b-value=2,000 s/mm^2). Each of the DWI scans included 4 volumes without diffusion weighting (b-value=0). We also collected one scan with 6 non-diffusion-weighted volumes and a reversed phase encoding direction (posterior-anterior) to correct for EPI distortions due to inhomogeneities in the magnetic field using FSL's topup tool (Andersson, Skare et al. 2003). Additional pre-processing is carried out using tools in FSL for motion and eddy current correction (Andersson and Sotiropoulos 2016). Data were manually checked for imaging artifacts and excessive dropped volumes. Given that subject motion can be especially problematic for the interpretation of group differences in DWI data (Yendiki, Koldewyn et al. 2014), data sets with mean slice-by-slice displacement > 3mm are excluded from further analysis.

bioRxiv preprint doi: https://doi.org/10.1101/2020.05.28.122499; this version posted May 29, 2020. The copyright holder for this preprint (which was not certified by peer review) is the author/funder, who has granted bioRxiv a license to display the preprint in perpetuity. It is made available under aCC-BY-NC-ND 4.0 International license.

For quantitative T1 mapping, we followed protocol developed by (Mezer, Yeatman et al. 2013). We acquired 4 spoiled gradient echo recalled images using two different flip angles (2 scans with 4° and 2 scans with 20°, all with TR = 14ms, TE = 2.3ms, and resolution of 1 mm^3). To correct the transmit coil inhomogeneity, we collected 4 spin echo inversion recovery scans with EPI read-out (SEIR-EPI), with TR 6500, TE 6.46, inversion times of 50, 400, 1200, 2400 ms, and 2mm^2 inplane resolution with a slice thickness of 4 mm. We then compared T1 fits estimated using the spoiled gradient echo images to fits estimated using the unbiased (Barral, Gudmundson et al. 2010, Mezer, Yeatman et al. 2013, Mezer, Rokem et al. 2016) SEIR-EPI images to characterize the inhomogeneity field and apply an appropriate correction to the biased, high resolution spoiled gradient echo recalled images.

Modeling white matter tissue properties

All diffusion and quantitative T1 data were aligned to a common anatomical reference in each subject's native, ACPC aligned space. Axonal water fraction and extra-axonal diffusivities were modeled using the white matter tract integrity (WMTI) model (Fieremans, Novikov et al. 2010, Fieremans, Jensen et al. 2011), after fitting the diffusion kurtosis model (Jensen, Helpern et al. 2005). WMTI and DKI fitting was implemented in DIPY (Garyfallidis, Brett et al. 2014). R1 maps were calculated by taking 1/T1 (seconds) for each voxel.

All values were then mapped onto fiber tracts identified for each subject using the Automated Fiber Quantification software package (Yeatman, Dougherty et al. 2012), after

bioRxiv preprint doi: https://doi.org/10.1101/2020.05.28.122499; this version posted May 29, 2020. The copyright holder for this preprint (which was not certified by peer review) is the author/funder, who has granted bioRxiv a license to display the preprint in perpetuity. It is made available under aCC-BY-NC-ND 4.0 International license.

initial generation of a whole-brain connectome using probabilistic tractography (MRtrix 3.0 (Tournier, Calamante et al. 2004)). Since the white matter tract integrity (WMTI) assumes that fibers are relatively well aligned (Fieremans, Jensen et al. 2011), we followed recommendations from previous work and restricted our analysis to voxels with fractional anisotropy values greater than 0.3 (Jensen, Stickley et al. 2017, Jensen, McKinnon et al. 2017, Chung, Fieremans et al. 2018). Specifically, voxels with fractional anisotropy below 0.3 were removed and WMTI metrics were interpolated at each point on each fiber, and then values were summarized along the fiber-tract core based on computing the median value across fiber nodes. Our previous work has demonstrated that summarizing values based on the median, rather than the mean, of WMTI metrics substantially increases the reliability of an individual's data (Huber 2018). Data with outlying values (greater than 4 standard deviations from the sample mean) in the white matter for any of the fitted metrics was excluded from further analysis. After excluding both outliers and individuals with excessive motion (>3mm, see above), the final data set included 109 sessions from 32 intervention subjects and 66 sessions from 27 non-intervention control subjects.

Statistical Analysis

Statistical analysis was carried out using software written in Matlab (*draft code link: https://github.com/yeatmanlab/BioBasis.git*). To assess change over the course of intervention, we first averaged the middle 80% of each tract to create a single estimate of each property for each subject and tract. We selected the middle portion to eliminate the influence of crossing fibers near cortical terminations, and to avoid potential partial volume

bioRxiv preprint doi: https://doi.org/10.1101/2020.05.28.122499; this version posted May 29, 2020. The copyright holder for this preprint (which was not certified by peer review) is the author/funder, who has granted bioRxiv a license to display the preprint in perpetuity. It is made available under aCC-BY-NC-ND 4.0 International license.

295 effects at the white matter / gray matter border. Mean tract values were then entered into a
296 linear mixed effects model, with fixed effects of intervention time and a random effect of
297 subject. For quantifying intervention effects, we prefer to use 'hours of intervention', since
298 this variable directly reflects the intervention 'dose'. For analyses including the control
299 subjects, who did not participate in an intervention of any kind, we substitute 'session' for
300 'hours'. Since sessions were held at regular intervals, the two variables were highly
301 correlated (Pearson's $r = 0.98$, $p < 0.001$).
302
303 **Results**
304
305 ***Diffusion MRI***
306
307 Significant changes in mean diffusivity (MD) were apparent throughout the white matter
308 in the intervention group (**Figure 1a-b**; tracts showing significant changes qFDR < 0.05).
309 In a group of age-matched control subjects who attended school as usual, we found no
310 significant changes in white matter diffusivity over the same time frame, and growth
311 estimates for the 16 pathways were distributed around zero (**Figure 1c**). A group
312 (intervention vs. non-intervention) by time (session number) interaction was significant (p
313 < 0.05, uncorrected) for the left arcuate and left inferior frontal-occipital fasciculus.
314

bioRxiv preprint doi: https://doi.org/10.1101/2020.05.28.122499; this version posted May 29, 2020. The copyright holder for this preprint (which was not certified by peer review) is the author/funder, who has granted bioRxiv a license to display the preprint in perpetuity. It is made available under aCC-BY-NC-ND 4.0 International license.

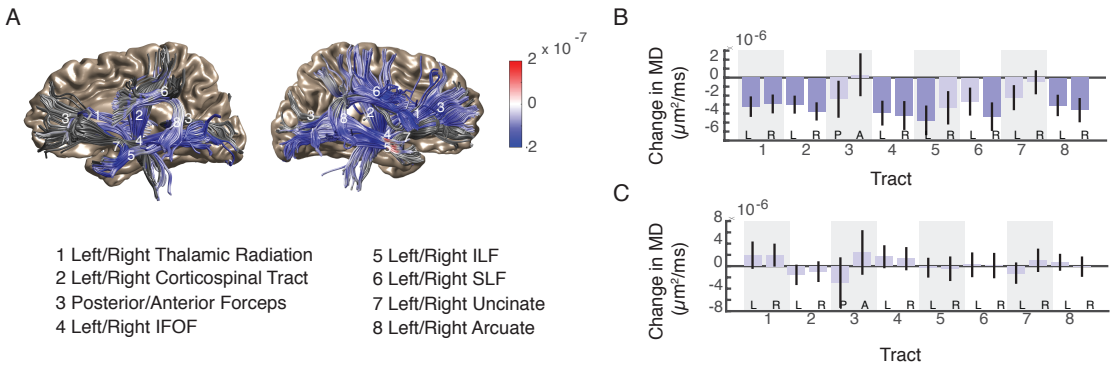

Figure 1. (A) White matter tracts are shown in two views (left hemisphere, right hemisphere) for an example subject. Color-coding is based on the coefficient from mean a linear mixed effects model predicting mean diffusivity (MD) values as a function of intervention hours at each location along each tract. Numeric labels correspond to the tract names listed at right. (B) Coefficients from a model (+/- 1 SE) substituting 'session' for 'hours of intervention', for the intervention group. Darker shaded bars reflect significant change (qFDR < 0.05). (C) Results for the control subjects, using the same statistical model as in (B). In the control group, growth estimates were distributed around zero with none of the tracts showing a significant change in MD over an 8-week period.

Although mean diffusivity is a highly sensitive measure (De Santis, Drakesmith et al. 2014, Huber 2018), it is not biologically specific. We next examined the effects of intervention on parameters estimated from the WMTI model: axonal water fraction (AWF) and extra-axonal mean diffusivity. As shown in **Figure 2**, intervention effects were limited to parameters associated with the extra-axonal space: Extra-axonal MD effects mirror the MD effects shown above. We saw no change in estimates of AWF over the intervention period.

bioRxiv preprint doi: https://doi.org/10.1101/2020.05.28.122499; this version posted May 29, 2020. The copyright holder for this preprint (which was not certified by peer review) is the author/funder, who has granted bioRxiv a license to display the preprint in perpetuity. It is made available under aCC-BY-NC-ND 4.0 International license.

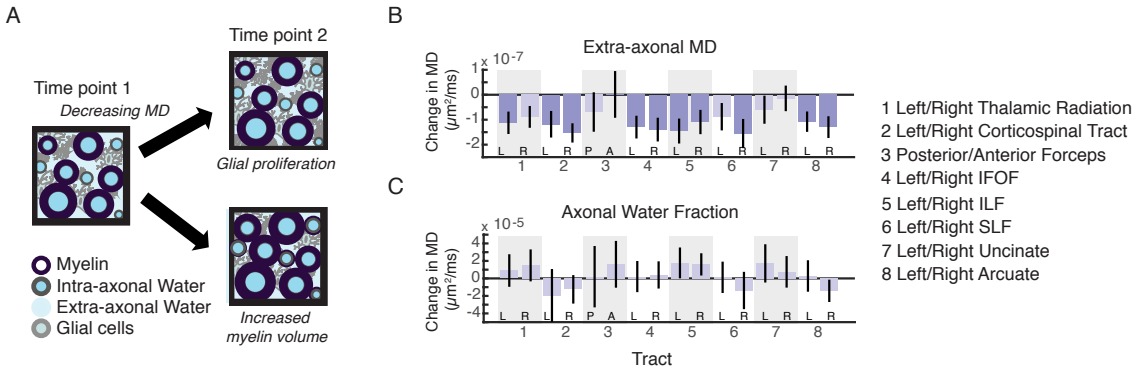

Figure 2. Microstructural modeling of white matter plasticity. (A) Illustration of two scenarios in which mean diffusivity would decline in a voxel: proliferation of glial cells within the extra axonal space (top) or increasing axon caliber and myelination (bottom). (B, C) Plots show coefficients from a linear mixed effects model predicting extra-axonal mean diffusivity and axon water fraction (AWF) from intervention time (in hours; random effect of subjects). Tracts showing significant change ($qFDR < 0.05$) are shaded.

We next examined how assumptions implemented in the WMTI model affect the results. Typically, the WMTI model assumes higher diffusivity within the extra-axonal space versus the intra-axonal space. This assumption is required for the model to converge on a single solution (Fieremans, Jensen et al. 2011). However, recent work has called this assumption into question (Jespersen, Olesen et al. 2018, Kunz, da Silva et al. 2018). Thus, to examine how this choice might affect our interpretation of the data, we perform a supplementary analysis in which we invert the assumed relationship between diffusivities (intra- greater than extra-axonal). Inverting the assumed relationship between diffusivities produced effects in intra-axonal diffusivity for the right IFOF and ILF, the left and right SLF, and the right Arcuate ($p < 0.05$, uncorrected) and rendered the remaining effects non-significant. Importantly, this change to the model does not affect our calculation of AWF

bioRxiv preprint doi: https://doi.org/10.1101/2020.05.28.122499; this version posted May 29, 2020. The copyright holder for this preprint (which was not certified by peer review) is the author/funder, who has granted bioRxiv a license to display the preprint in perpetuity. It is made available under aCC-BY-NC-ND 4.0 International license.

(Fieremans, Jensen et al. 2011), and so these results are the same under either set of assumptions: We find no detectable difference in AWF over the course of the intervention.

Quantitative T1

The effects observed in the diffusion MRI data set suggest that learning related changes in the white matter reflect increased hindrance of diffusion within the extra-axonal space, rather than an increase in the total volume of myelin. We next test this idea using using a separate qMRI data set. R1 measurements reflect both the total volume of tissue in a region, and the molecular composition, such as lipid and iron, of that tissue (Mezer, Yeatman et al. 2013, Stuber, Morawski et al. 2014, Filo, Shtangel et al. 2019). A decrease in the volume of myelinated tissue (or, an increase in water) within a voxel would be associated with lower measured R1 values, while an increase in myelinated tissue would be associated with elevated R1 measurements. Consistent with the interpretation suggested by the DKI and WMTI fits, we see no measureable change in R1 over the course of the intervention period in either group ($qFDR < 0.05$, **Figure 3a-b**), even when using a more lenient statistical threshold ($p < 0.05$, uncorrected). Meanwhile, tract-average R1 values measured at baseline in the anterior callosal tract, left arcuate, and left and right ILF correlate with individual differences in reading skill prior to the start of the intervention ($p < 0.05$, uncorrected**, Figure 3c**), confirming that R1 is sensitive to behaviorally relevant properties of the white matter.

bioRxiv preprint doi: https://doi.org/10.1101/2020.05.28.122499; this version posted May 29, 2020. The copyright holder for this preprint (which was not certified by peer review) is the author/funder, who has granted bioRxiv a license to display the preprint in perpetuity. It is made available under aCC-BY-NC-ND 4.0 International license.

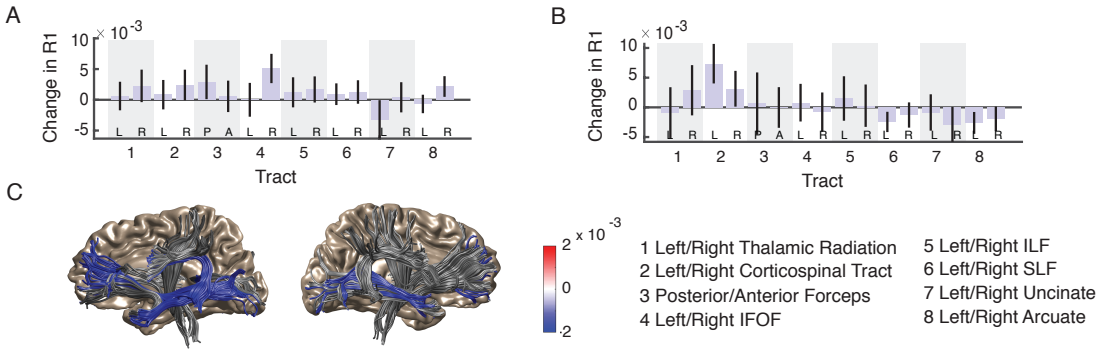

Figure 3. Quantitative R1 values do not show significant change over the intervention period in the intervention group (A), or the non-intervention control group (B). Bar plots show coefficients from a linear mixed effects model predicting R1 from intervention time (session; random effect of subject). (C) Baseline R1 values correlate pre-intervention reading performance. Color coding reflects the coefficient from a linear model predicting tract-average R1 values from (age-standardized) pre-intervention reading scores. Regions without a significant ($p < 0.05$) relationship to behavior are colored gray.

Discussion

Here we use diffusion MRI and a model derived from diffusion kurtosis imaging (Fieremans, Jensen et al. 2011), alongside quantitative R1 (1/T1 relaxation time) measurements, to examine whether microstructural changes during a successful reading intervention are best interpreted as rapid, experience-dependent changes in the volume of axons and myelin, or as changes in diffusivity within the extra- and/or intra-axonal space. Our results support the latter interpretation. While we observed systematic changes in diffusivity during the intervention, we failed to detect a longitudinal change in restricted fraction of the diffusion signal (interpreted as axonal water fraction, AWF), which would

bioRxiv preprint doi: https://doi.org/10.1101/2020.05.28.122499; this version posted May 29, 2020. The copyright holder for this preprint (which was not certified by peer review) is the author/funder, who has granted bioRxiv a license to display the preprint in perpetuity. It is made available under aCC-BY-NC-ND 4.0 International license.

393 be expected to arise from a sufficiently large change in myelination (Jelescu, Zurek et al.
394 2016), or a change in axon caliber. Although we interpret this null result cautiously, we
395 have previously demonstrated that AWF can be estimated reliably in this age group, and
396 that AWF is highly sensitive to maturational changes that occur over the timescale of years
397 (Huber 2018). Consistent with the diffusion MRI results, we did not observe a change in
398 quantitative R1 values over the intervention period. However, in the same individuals (both
399 intervention and non-intervention control subjects), we found that R1 was correlated with
400 pre-intervention reading skill. This argues that R1 measurements capture behaviorally
401 relevant variation in white matter microstructure that are distinct from the biological
402 mechanisms associated with short-term plasticity and learning during an intensive
403 intervention.
404
405 We previously (Huber 2018) reported changes in mean diffusivity alongside growth in
406 reading skills during an intensive reading intervention. If these effects indeed reflect
407 properties of the extra-axonal space, what is the link to behavior? A systematic reduction
408 in extra-axonal diffusivity, without corresponding changes in axonal water fraction or
409 quantitative R1, could result from an increase in cell membranes hindering diffusion within
410 the extra-axonal space, without a corresponding change in the total volume of that space.
411 This might reflect proliferation of oligodendrocyte precursor cells (OPC), as seen in
412 previous animal work (Gibson, Purger et al. 2014), although extra-axonal diffusivity
413 estimates could also be influenced by changes in the size or distribution of astrocytes
414 (Sampaio-Baptista and Johansen-Berg 2017, Sepehrband, Cabeen et al. 2018).
415

bioRxiv preprint doi: https://doi.org/10.1101/2020.05.28.122499; this version posted May 29, 2020. The copyright holder for this preprint (which was not certified by peer review) is the author/funder, who has granted bioRxiv a license to display the preprint in perpetuity. It is made available under aCC-BY-NC-ND 4.0 International license.

The relationship between higher-level cognitive function, axonal, glial and vascular properties is likely to be complex, and the process of maintaining and optimizing signaling properties involves a number of distinct biological phenomena that operate over different time scales. However, it is increasingly clear that activation and proliferation of glial cells and their precursors is vital not only for maintenance of active connections within a circuit, but also for the optimization of signaling properties. For example, oligodendrocytes participate in myelin maintenance, repair, and use-related plasticity throughout the lifespan (reviewed in (Nave 2010)), and have been shown to regulate axon caliber directly, independent of myelination (Sanchez, Hassinger et al. 1996). This mechanism could theoretically support fast, activity-dependent changes in signaling efficiency and coordination. Neural activity, in turn, appears to promote oligodendrocyte precursor proliferation (Barres and Raff 1993), perhaps increasing the potential malleability of highly active circuits. Although the link between these biological phenomena and learning is not yet well understood, animal models have demonstrated a critical role of glia for brain function in health, and their dysfunction in disease states (Barres 2008). Studies employing longitudinal measurements, coupled with increasingly sophisticated imaging and modeling techniques, hold promise for revealing the interplay among distinct biological processes that support learning and cognition. Our findings highlight the importance of considering the often-ignored contribution of glial cells to diffusion measurements and associated cognitive functions in humans across the lifespan.

Linking the diffusion process to tissue biology requires making certain assumptions about the factors that contribute to measured diffusion signals (Novikov, Kiselev et al. 2018).

bioRxiv preprint doi: https://doi.org/10.1101/2020.05.28.122499; this version posted May 29, 2020. The copyright holder for this preprint (which was not certified by peer review) is the author/funder, who has granted bioRxiv a license to display the preprint in perpetuity. It is made available under aCC-BY-NC-ND 4.0 International license.

The WMTI model used here assumes well-aligned fibers as its inputs (Fieremans, Novikov et al. 2010). We have tried to assure that this assumption is met in our analysis by sampling voxels with fractional anisotropy values that fall within a range for which the model has been validated (Jensen, McKinnon et al. 2017, Chung, Fieremans et al. 2018). In order to fit the WMTI model with a single solution, one must further assume a higher rate of diffusivity within either the intra-axonal or extra-axonal space for a given region of interest. Previous work has validated the assumption of higher intrinsic diffusivity within the extra-axonal-space (Guglielmetti, Veraart et al. 2016, Jelescu, Zurek et al. 2016), although recent work has called this assumption into question (i.e., intra-axonal diffusivity may be greater than extra-axonal diffusivity; (Jespersen, Olesen et al. 2018, Kunz, da Silva et al. 2018)). Importantly, our calculation of AWF is robust, and does not depend on this assumption; thus, our main finding of stable AWF does not depend how the relative diffusivities are constrained. However, this choice does determine whether intervention-driven changes in diffusivity are attributed to the intra- versus extra-axonal space, in some cases. Although it is less clear what mechanism would alter the intrinsic diffusivity of the intra-axonal space over the timescales considered here, it is important to note that we cannot differentiate between these scenarios based solely on the WMTI model. Thus, our modeling results should not be interpreted as conclusive evidence for any specific biological mechanism.

Maturational differences in diffusion within the white matter reflect pruning of connections and changes in myelination that occur over the timescale of years (Chang, Owen et al. 2015, Jelescu, Veraart et al. 2015), which may in turn influence reading outcomes (Yeatman, Dougherty et al. 2012). The current data support the notion that short-term

bioRxiv preprint doi: https://doi.org/10.1101/2020.05.28.122499; this version posted May 29, 2020. The copyright holder for this preprint (which was not certified by peer review) is the author/funder, who has granted bioRxiv a license to display the preprint in perpetuity. It is made available under aCC-BY-NC-ND 4.0 International license.

462 changes in diffusion properties reflect an initial stage of the learning process, but the
463 connection between rapid changes and long-term remodeling of axons and myelin is
464 currently unknown. Resolving the relationship between learning and plasticity at temporal
465 scales ranging from hours (Sagi, Tavor et al. 2012, Hofstetter, Tavor et al. , Hofstetter,
466 Friedmann et al.), to days (Huber 2018), to years (Yeatman, Dougherty et al. 2012, Wang,
467 Mauer et al. 2017), will require research aimed at forging a tighter link between education
468 and neuroscience.
469
470

bioRxiv preprint doi: https://doi.org/10.1101/2020.05.28.122499; this version posted May 29, 2020. The copyright holder for this preprint (which was not certified by peer review) is the author/funder, who has granted bioRxiv a license to display the preprint in perpetuity. It is made available under aCC-BY-NC-ND 4.0 International license.

References

Alexander, A. L., J. E. Lee, M. Lazar and A. S. Field (2007). "Diffusion tensor imaging of the brain." Neurotherapeutics **4**(3): 316-329.

Alexander, D. C., T. B. Dyrby, M. Nilsson and H. Zhang (2019). "Imaging brain microstructure with diffusion MRI: practicality and applications." NMR Biomed **32**(4): e3841.

Andersson, J. L., S. Skare and J. Ashburner (2003). "How to correct susceptibility distortions in spin-echo echo-planar images: application to diffusion tensor imaging." Neuroimage **20**(2): 870-888.

Andersson, J. L. and S. N. Sotiropoulos (2016). "An integrated approach to correction for off-resonance effects and subject movement in diffusion MR imaging." Neuroimage **125**: 1063-1078.

Barral, J. K., E. Gudmundson, N. Stikov, M. Etezadi-Amoli, P. Stoica and D. G. Nishimura (2010). "A robust methodology for in vivo T1 mapping." Magn Reson Med **64**(4): 1057-1067.

Barres, B. A. (2008). "The mystery and magic of glia: a perspective on their roles in health and disease." Neuron **60**(3): 430-440.

Barres, B. A. and M. C. Raff (1993). "Proliferation of oligodendrocyte precursor cells depends on electrical activity in axons." Nature **361**(6409): 258-260.

Basser, P. J. and C. Pierpaoli (1996). "Microstructural and physiological features of tissues elucidated by quantitative-diffusion-tensor MRI." J Magn Reson B **111**(3): 209-219.

bioRxiv preprint doi: https://doi.org/10.1101/2020.05.28.122499; this version posted May 29, 2020. The copyright holder for this preprint (which was not certified by peer review) is the author/funder, who has granted bioRxiv a license to display the preprint in perpetuity. It is made available under aCC-BY-NC-ND 4.0 International license.

494 Bell, N. (2007). Seeing stars. San Luis Obispo, CA, Gander.

495 Benitez, A., E. Fieremans, J. H. Jensen, M. F. Falangola, A. Tabesh, S. H. Ferris and J. A.
496 Helpern (2014). "White matter tract integrity metrics reflect the vulnerability of late-
497 myelinating tracts in Alzheimer's disease." Neuroimage Clin **4**: 64-71.

498 Blumenfeld-Katzir, T., O. Pasternak, M. Dagan and Y. Assaf (2011). "Diffusion MRI of
499 structural brain plasticity induced by a learning and memory task." PLoS One **6**(6):
500 e20678.

501 Cercignani, M. and S. Bouyagoub (2018). "Brain microstructure by multi-modal MRI:
502 Is the whole greater than the sum of its parts?" Neuroimage **182**: 117-127.

503 Chang, Y. S., J. P. Owen, N. J. Pojman, T. Thieu, P. Bukshpun, M. L. Wakahiro, J. I. Berman,
504 T. P. Roberts, S. S. Nagarajan, E. H. Sherr and P. Mukherjee (2015). "White Matter
505 Changes of Neurite Density and Fiber Orientation Dispersion during Human Brain
506 Maturation." PLoS One **10**(6): e0123656.

507 Chung, S., E. Fieremans, N. E. Kucukboyaci, X. Wang, C. J. Morton, D. S. Novikov, J. F.
508 Rath and Y. W. Lui (2018). "Working Memory And Brain Tissue Microstructure: White
509 Matter Tract Integrity Based On Multi-Shell Diffusion MRI." Sci Rep **8**(1): 3175.

510 De Santis, S., M. Drakesmith, S. Bells, Y. Assaf and D. K. Jones (2014). "Why diffusion
511 tensor MRI does well only some of the time: variance and covariance of white matter
512 tissue microstructure attributes in the living human brain." Neuroimage **89**: 35-44.

513 Engvig, A., A. M. Fjell, L. T. Westlye, T. Moberget, O. Sundseth, V. A. Larsen and K. B.
514 Walhovd (2012). "Memory training impacts short-term changes in aging white
515 matter: a longitudinal diffusion tensor imaging study." Hum Brain Mapp **33**(10):
516 2390-2406.

bioRxiv preprint doi: https://doi.org/10.1101/2020.05.28.122499; this version posted May 29, 2020. The copyright holder for this preprint (which was not certified by peer review) is the author/funder, who has granted bioRxiv a license to display the preprint in perpetuity. It is made available under aCC-BY-NC-ND 4.0 International license.

517 Falangola, M. F., D. N. Guilfoyle, A. Tabesh, E. S. Hui, X. Nie, J. H. Jensen, S. V. Gerum, C.
518 Hu, J. LaFrancois, H. R. Collins and J. A. Helpern (2014). "Histological correlation of
519 diffusional kurtosis and white matter modeling metrics in cuprizone-induced corpus
520 callosum demyelination." NMR Biomed **27**(8): 948-957.
521 Fieremans, E., A. Benitez, J. H. Jensen, M. F. Falangola, A. Tabesh, R. L. Deardorff, M. V.
522 Spampinato, J. S. Babb, D. S. Novikov, S. H. Ferris and J. A. Helpern (2013). "Novel white
523 matter tract integrity metrics sensitive to Alzheimer disease progression." AJNR Am J
524 Neuroradiol **34**(11): 2105-2112.
525 Fieremans, E., J. H. Jensen and J. A. Helpern (2011). "White matter characterization
526 with diffusional kurtosis imaging." Neuroimage **58**(1): 177-188.
527 Fieremans, E., D. S. Novikov, J. H. Jensen and J. A. Helpern (2010). "Monte Carlo study
528 of a two-compartment exchange model of diffusion." NMR Biomed **23**(7): 711-724.
529 Filo, S., O. Shtangel, N. Salamon, A. Kol, B. Weisinger, S. Shifman and A. A. Mezer
530 (2019). "Disentangling molecular alterations from water-content changes in the
531 aging human brain using quantitative MRI." Nat Commun **10**(1): 3403.
532 Garyfallidis, E., M. Brett, B. Amirbekian, A. Rokem, S. van der Walt, M. Descoteaux, I.
533 Nimmo-Smith and C. Dipy (2014). "Dipy, a library for the analysis of diffusion MRI
534 data." Front Neuroinform **8**: 8.
535 Genc, S., C. B. Malpas, S. K. Holland, R. Beare and T. J. Silk (2017). "Neurite density
536 index is sensitive to age related differences in the developing brain." Neuroimage
537 **148**: 373-380.
538 Gibson, E. M., D. Purger, C. W. Mount, A. K. Goldstein, G. L. Lin, L. S. Wood, I. Inema, S.
539 E. Miller, G. Bieri, J. B. Zuchero, B. A. Barres, P. J. Woo, H. Vogel and M. Monje (2014).

bioRxiv preprint doi: https://doi.org/10.1101/2020.05.28.122499; this version posted May 29, 2020. The copyright holder for this preprint (which was not certified by peer review) is the author/funder, who has granted bioRxiv a license to display the preprint in perpetuity. It is made available under aCC-BY-NC-ND 4.0 International license.

"Neuronal activity promotes oligodendrogenesis and adaptive myelination in the mammalian brain." Science **344**(6183): 1252304.

Guglielmetti, C., J. Veraart, E. Roelant, Z. Mai, J. Daans, J. Van Audekerke, M. Naeyaert, G. Vanhoutte, Y. P. R. Delgado, J. Praet, E. Fieremans, P. Ponsaerts, J. Sijbers, A. Van der Linden and M. Verhoye (2016). "Diffusion kurtosis imaging probes cortical alterations and white matter pathology following cuprizone induced demyelination and spontaneous remyelination." Neuroimage **125**: 363-377.

Hofstetter, S., N. Friedmann and Y. Assaf (2017). "Rapid language-related plasticity: microstructural changes in the cortex after a short session of new word learning." Brain Struct Funct **222**(3): 1231-1241.

Hofstetter, S., I. Tavor, S. Tzur Moryosef and Y. Assaf (2013). "Short-term learning induces white matter plasticity in the fornix." J Neurosci **33**(31): 12844-12850.

Huber, E., Donnelly, P.M., Rokem, A., Yeatman, J.D. (2018). "Rapid and widespread white matter plasticity during an intensive reading intervention." Nature Communications.

Huber, E., Henriques, R.N., Owen, J.P., Rokem, A., Yeatman, J.D. (2018). "Applying biophysical models to understand the role of white matter in cognitive development." bioRxiv.

Jelescu, I. O. and M. D. Budde (2017). "Design and validation of diffusion MRI models of white matter." Front Phys **28**.

Jelescu, I. O., J. Veraart, V. Adisetiyo, S. S. Milla, D. S. Novikov and E. Fieremans (2015). "One diffusion acquisition and different white matter models: how does

bioRxiv preprint doi: https://doi.org/10.1101/2020.05.28.122499; this version posted May 29, 2020. The copyright holder for this preprint (which was not certified by peer review) is the author/funder, who has granted bioRxiv a license to display the preprint in perpetuity. It is made available under aCC-BY-NC-ND 4.0 International license.

562 microstructure change in human early development based on WMTI and NODDI?"
563 Neuroimage **107**: 242-256.
564 Jelescu, I. O., M. Zurek, K. V. Winters, J. Veraart, A. Rajaratnam, N. S. Kim, J. S. Babb, T.
565 M. Shepherd, D. S. Novikov, S. G. Kim and E. Fieremans (2016). "In vivo quantification
566 of demyelination and recovery using compartment-specific diffusion MRI metrics
567 validated by electron microscopy." Neuroimage **132**: 104-114.
568 Jensen, A., T. Stickley, W. Torrissen and K. Stigmar (2017). "Arts on prescription in
569 Scandinavia: a review of current practice and future possibilities." Perspect Public
570 Health **137**(5): 268-274.
571 Jensen, J. H., J. A. Helpern, A. Ramani, H. Lu and K. Kaczynski (2005). "Diffusional
572 kurtosis imaging: the quantification of non-gaussian water diffusion by means of
573 magnetic resonance imaging." Magn Reson Med **53**(6): 1432-1440.
574 Jensen, J. H., E. T. McKinnon, G. R. Glenn and J. A. Helpern (2017). "Evaluating kurtosis-
575 based diffusion MRI tissue models for white matter with fiber ball imaging." NMR
576 Biomed **30**(5).
577 Jespersen, S. N., J. L. Olesen, B. Hansen and N. Shemesh (2018). "Diffusion time
578 dependence of microstructural parameters in fixed spinal cord." Neuroimage **182**:
579 329-342.
580 Kelm, N. D., K. L. West, R. P. Carson, D. F. Gochberg, K. C. Ess and M. D. Does (2016).
581 "Evaluation of diffusion kurtosis imaging in ex vivo hypomyelinated mouse brains."
582 Neuroimage **124**(Pt A): 612-626.
583 Kunz, N., A. R. da Silva and I. O. Jelescu (2018). "Intra- and extra-axonal axial
584 diffusivities in the white matter: Which one is faster?" Neuroimage **181**: 314-322.

bioRxiv preprint doi: https://doi.org/10.1101/2020.05.28.122499; this version posted May 29, 2020. The copyright holder for this preprint (which was not certified by peer review) is the author/funder, who has granted bioRxiv a license to display the preprint in perpetuity. It is made available under aCC-BY-NC-ND 4.0 International license.

585 Le Bihan, D. (1995). "Molecular diffusion, tissue microdynamics and microstructure."
586 NMR Biomed **8**(7-8): 375-386.
587 Lerch, J. P., A. P. Yiu, A. Martinez-Canabal, T. Pekar, V. D. Bohbot, P. W. Frankland, R.
588 M. Henkelman, S. A. Josselyn and J. G. Sled (2011). "Maze training in mice induces MRI-
589 detectable brain shape changes specific to the type of learning." Neuroimage **54**(3):
590 2086-2095.
591 Mamiya, P. C., T. L. Richards, B. P. Coe, E. E. Eichler and P. K. Kuhl (2016). "Brain white
592 matter structure and COMT gene are linked to second-language learning in adults."
593 Proc Natl Acad Sci U S A **113**(26): 7249-7254.
594 Mezer, A., A. Rokem, S. Berman, T. Hastie and B. A. Wandell (2016). "Evaluating
595 quantitative proton-density-mapping methods." Hum Brain Mapp **37**(10): 3623-
596 3635.
597 Mezer, A., J. D. Yeatman, N. Stikov, K. N. Kay, N. J. Cho, R. F. Dougherty, M. L. Perry, J.
598 Parvizi, H. Hua le, K. Butts-Pauly and B. A. Wandell (2013). "Quantifying the local
599 tissue volume and composition in individual brains with magnetic resonance
600 imaging." Nat Med **19**(12): 1667-1672.
601 Nave, K. A. (2010). "Myelination and support of axonal integrity by glia." Nature
602 **468**(7321): 244-252.
603 Novikov, D. S., V. G. Kiselev and S. N. Jespersen (2018). "On modeling." Magn Reson
604 Med **79**(6): 3172-3193.
605 Sagi, Y., I. Tavor, S. Hofstetter, S. Tzur-Moryosef, T. Blumenfeld-Katzir and Y. Assaf
606 (2012). "Learning in the fast lane: new insights into neuroplasticity." Neuron **73**(6):
607 1195-1203.

bioRxiv preprint doi: https://doi.org/10.1101/2020.05.28.122499; this version posted May 29, 2020. The copyright holder for this preprint (which was not certified by peer review) is the author/funder, who has granted bioRxiv a license to display the preprint in perpetuity. It is made available under aCC-BY-NC-ND 4.0 International license.

608 Sampaio-Baptista, C. and H. Johansen-Berg (2017). "White Matter Plasticity in the
609 Adult Brain." Neuron **96**(6): 1239-1251.
610 Sampaio-Baptista, C., A. A. Khrapitchev, S. Foxley, T. Schlagheck, J. Scholz, S. Jbabdi, G.
611 C. DeLuca, K. L. Miller, A. Taylor, N. Thomas, J. Kleim, N. R. Sibson, D. Bannerman and
612 H. Johansen-Berg (2013). "Motor skill learning induces changes in white matter
613 microstructure and myelination." J Neurosci **33**(50): 19499-19503.
614 Sanchez, I., L. Hassinger, P. A. Paskevich, H. D. Shine and R. A. Nixon (1996).
615 "Oligodendroglia regulate the regional expansion of axon caliber and local
616 accumulation of neurofilaments during development independently of myelin
617 formation." J Neurosci **16**(16): 5095-5105.
618 Sepehrband, F., R. P. Cabeen, J. Choupan, G. Barisano, M. Law and A. W. Toga (2018).
619 "A systematic bias in DTI findings." bioRxiv.
620 Stuber, C., M. Morawski, A. Schafer, C. Labadie, M. Wahnert, C. Leuze, M. Streicher, N.
621 Barapatre, K. Reimann, S. Geyer, D. Spemann and R. Turner (2014). "Myelin and iron
622 concentration in the human brain: a quantitative study of MRI contrast." Neuroimage
623 **93 Pt 1**: 95-106.
624 Takemura, H., S. Ogawa, A. A. Mezer, H. Horiguchi, A. Miyazaki, K. Matsumoto, K.
625 Shikishima, T. Nakano and Y. Masuda (2019). "Diffusivity and quantitative T1 profile
626 of human visual white matter tracts after retinal ganglion cell damage." Neuroimage
627 Clin **23**: 101826.
628 Taubert, M., B. Draganski, A. Anwander, K. Muller, A. Horstmann, A. Villringer and P.
629 Ragert (2010). "Dynamic properties of human brain structure: learning-related

bioRxiv preprint doi: https://doi.org/10.1101/2020.05.28.122499; this version posted May 29, 2020. The copyright holder for this preprint (which was not certified by peer review) is the author/funder, who has granted bioRxiv a license to display the preprint in perpetuity. It is made available under aCC-BY-NC-ND 4.0 International license.

630 changes in cortical areas and associated fiber connections." J Neurosci **30**(35): 11670-
631 11677.
632 Tournier, J. D., F. Calamante, D. G. Gadian and A. Connelly (2004). "Direct estimation
633 of the fiber orientation density function from diffusion-weighted MRI data using
634 spherical deconvolution." Neuroimage **23**(3): 1176-1185.
635 Travis, K. E., M. R. H. Castro, S. Berman, C. K. Dodson, A. A. Mezer, M. Ben-Shachar and
636 H. M. Feldman (2019). "More than myelin: Probing white matter differences in
637 prematurity with quantitative T1 and diffusion MRI." Neuroimage Clin **22**: 101756.
638 Walhovd, K. B., H. Johansen-Berg and R. T. Karadottir (2014). "Unraveling the secrets
639 of white matter--bridging the gap between cellular, animal and human imaging
640 studies." Neuroscience **276**: 2-13.
641 Wang, Y., M. V. Mauer, T. Raney, B. Peysakhovich, B. L. C. Becker, D. D. Sliva and N.
642 Gaab (2017). "Development of Tract-Specific White Matter Pathways During Early
643 Reading Development in At-Risk Children and Typical Controls." Cereb Cortex **27**(4):
644 2469-2485.
645 Yeatman, J. D., R. F. Dougherty, M. Ben-Shachar and B. A. Wandell (2012).
646 "Development of white matter and reading skills." Proc Natl Acad Sci U S A **109**(44):
647 E3045-3053.
648 Yeatman, J. D., R. F. Dougherty, N. J. Myall, B. A. Wandell and H. M. Feldman (2012).
649 "Tract profiles of white matter properties: automating fiber-tract quantification."
650 PLoS One **7**(11): e49790.

bioRxiv preprint doi: https://doi.org/10.1101/2020.05.28.122499; this version posted May 29, 2020. The copyright holder for this preprint (which was not certified by peer review) is the author/funder, who has granted bioRxiv a license to display the preprint in perpetuity. It is made available under aCC-BY-NC-ND 4.0 International license.

651 Yendiki, A., K. Koldewyn, S. Kakunoori, N. Kanwisher and B. Fischl (2014). "Spurious
652 group differences due to head motion in a diffusion MRI study." Neuroimage **88**: 79-
653 90.

654